Formation, Characterization, and Magnetic Properties of Fe_3O_4 Nanowires Encapsulated in Carbon Microtubes

Liqiang Xu,[†,‡] Wanqun Zhang,[‡] Yanwei Ding,[†] Yiya Peng,[‡] Shuyuan Zhang,[†] Weichao Yu,[†] and Yitai Qian*[,†,‡]

Structure Research Laboratory and Department of Chemistry, University of Science and Technology of China, Hefei, Anhui 230026

Received: February 15, 2004; In Final Form: May 10, 2004

Iron oxide (Fe_3O_4) nanowires encapsulated in carbon microtubes (defined as "CIOs") with a diameter range of 150−1500 nm, and lengths up to 6 um were obtained by pyrolyzing an ethanol/ferrocene mixture in an autoclave at 600 °C. The inner Fe_3O_4 nanowires (defined as "IOs") are single crystalline with a diameter range of 55−750 nm. Magnetic hysteresis loop measurements show that the CIOs display ferromagnetic properties at room temperature. In addition, carbon microtubes (CMTs) were obtained after the inside IOs were dissolved by aqueous HCl acid.

Introduction

Since the discovery of carbon nanotubes in 1991,[1] extensive research has been concentrated on the encapsulation of foreign materials inside hollow cavities of carbon nanotubes owing to their significant electronic, magnetic, and nonlinear optical properties, as well as to a variety of industrial applications as catalysts, electronic devices, biosensors, and improved magnetic tapes,[2−6] and diversified approaches have been reported for the synthesis of foreign materials encapsulated in carbon nanotubes, such as capillary action,[7] wet chemical method,[8] arc-discharge technique,[9] template carbonization method,[10] catalyzed hydrocarbon pyrolysis,[11−13] spray pyrolysis,[14] and condensed phase electrolysis.[15] As ferromagnetic materials (e.g., Fe, Ni, Co) encapsulated in carbon nanotubes may prove possible to develop magnetic data storage devices and toners and inks for xerography and magnetic resonance imaging,[16] various materials including iron, iron oxide, cobalt, and $CoFe_2O_4$ encapsulated in carbon nanotubes have been prepared.[17−23] However, the potential of foreign materials encapsulated in carbon nanotubes as devices is significantly hampered due to their nanometer-size diameters (typically 1−100 nm); therefore, carbon micrometer tubes with materials encapsulated in their hollow cavities might be an alternative object more capable of shedding additional light on various physical and chemical phenomena than those of materials encapsulated in carbon nanotubes. In this study, we introduce a Co-pyrolysis method for the fabrication of CIOs by pyrolyzing an ethanol/ferrocene mixture in a stainless steel autoclave at 600 °C. The as-prepared CIOs have a diameter range of 150−1500 nm and lengths up to 6 μm, and the encapsulated IOs are single crystalline. Magnetic hysteresis loop measurements show that the as-obtained CIOs display ferromagnetic properties at room temperature. In addition, carbon microtubes were obtained after the inside Fe_3O_4 nanowires were dissolved by aqueous HCl acid. The main advantage of this synthesis method over the others is that it provides a low-cost and convenient way to prepare straight CIOs and CMTs without using any specific template and encapsulation process.

Experimental Section

Sample Preparation. In a typical procedure, ferrocene (1.0 g) and absolute ethanol (18 mL) were loaded into a stainless steel autoclave of 20 mL capacity. The autoclave was sealed and put into an electronic furnace at 100 °C; then the temperature of the furnace was increased to 600 °C over 50 min and maintained at 600 °C under ca. 15 MPa for 16 h and then allowed to cool to room temperature naturally. It was found that the final products in the autoclave included many dark precipitates, a little volume of H_2O, and some residual gases. The dark precipitates stuck on the interior surface of the wall of the autoclave were collected and divided into two parts: one part was washed with distilled water and absolute ethanol several times to obtain the CIOs; the other parts were heated in dilute HCl acidic solution at 80 °C for 24 h to obtain carbon microtubes. After that, the two samples were dried in a vacuum box at 60 °C for 4 h and were collected for characterization.

Sample Characterization. X-ray powder diffraction (XRD) patterns of the two samples with different treatments were recorded on a Philips X'pert diffractometer with Cu Kα radiation ($\lambda = 1.541\,78$ Å). The Raman spectrum was recorded at ambient temperature on a SPEX 1403 spectrometer with an argon-ion laser at an excitation wavelength of 514.5 nm. The morphology, structure, and compositions of the CIOs and CMTs were examined with field emission scanning electron microscopy (FSEM, JEOL JSM-6300F), FSEM-energy-dispersive X-ray analysis, transmission electron microscopy (TEM, HITACHI 800), and high-resolution TEM (HRTEM, JEOL 2010 using an accelerating voltage of 200 kV). Before the FSEM, TEM, and HRTEM analyses, the samples were ultrasonicated in ethanol and were mounted on a copper disk or copper net. The Mössbauer spectrum was recorded on the MS-500 spectrometer (Oxford Co.) with a ^{57}Co source in a Pd matrix on a constant acceleration drive at room temperature and zero fields. Hyperfine interaction parameters were derived from the use of a Newton−Gauss method. The magnetic measurement of the products was carried out in a vibrating sample magnetometer

* To whom correspondence should be addressed. Telephone: +86-551-3602942. Fax: +86-551-3607402. E-mail: xulq@mail.ustc.edu.cn.
† Structure Research Laboratory.
‡ Department of Chemistry.

10.1021/jp049318u CCC: $27.50
Published on Web 06/18/2004

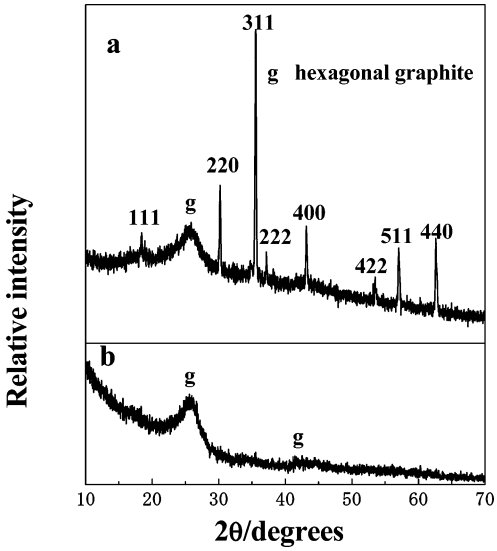

Figure 1. XRD patterns of the products with different treatments. (a) Washed with distilled water and ethanol for several times. (b) After aqueous HCl acid solutions treatment then washed with distilled water and ethanol for several times.

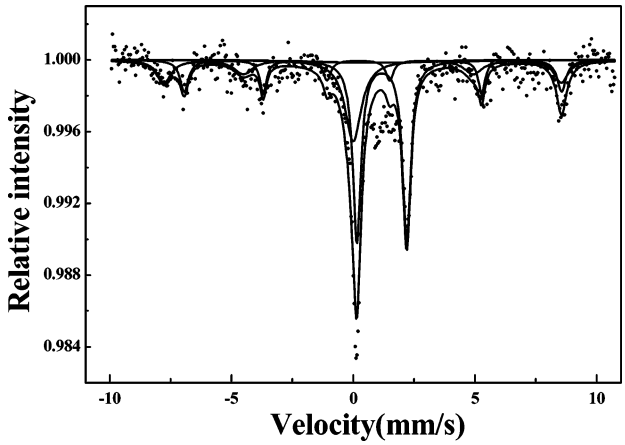

Figure 2. Mössbauer spectrum of the as-obtained CIOs measured at room temperature.

(VSM) (BHV-55, Riken, Japan). Magnetic hysteresis loops were recorded at room temperature by first saturating the sample in a field of 10 000 Oe, and then the saturation magnetization (M_s), the remanent magnetization (M_r), and the coercivity (H_c) were determined for the sample.

Results and Discussion

Figure 1 shows the powder X-ray diffraction (XRD) patterns of the two samples. Figure 1a is the XRD pattern of the product after washing with distilled water and ethanol. According to the reflection peaks in this figure, the main phases included in the products can be indexed as face-centered cubic (fcc) Fe_3O_4 (JCPDS Card no. 19-629) and hexagonal graphite (JCPDS Card no. 48-1487), respectively. Figure 1b shows the XRD pattern of the product after heated in diluted HCl acidic solutions, which can be indexed as pure hexagonal graphite. Compared with the two phases shown in Figure 1, it is clear that the Fe_3O_4 phase has a higher crystallinity than that of the carbon phase. To further ascertain the phase of the iron oxides, the Mössbauer spectrum of the CIOs has been measured and the result is shown in Figure 2. The corresponding hyperfine parameters are found to be 487 and 462 KOe and 0.28 and 0.68 mm/s with respect to iron metal, respectively, which agree well with values found

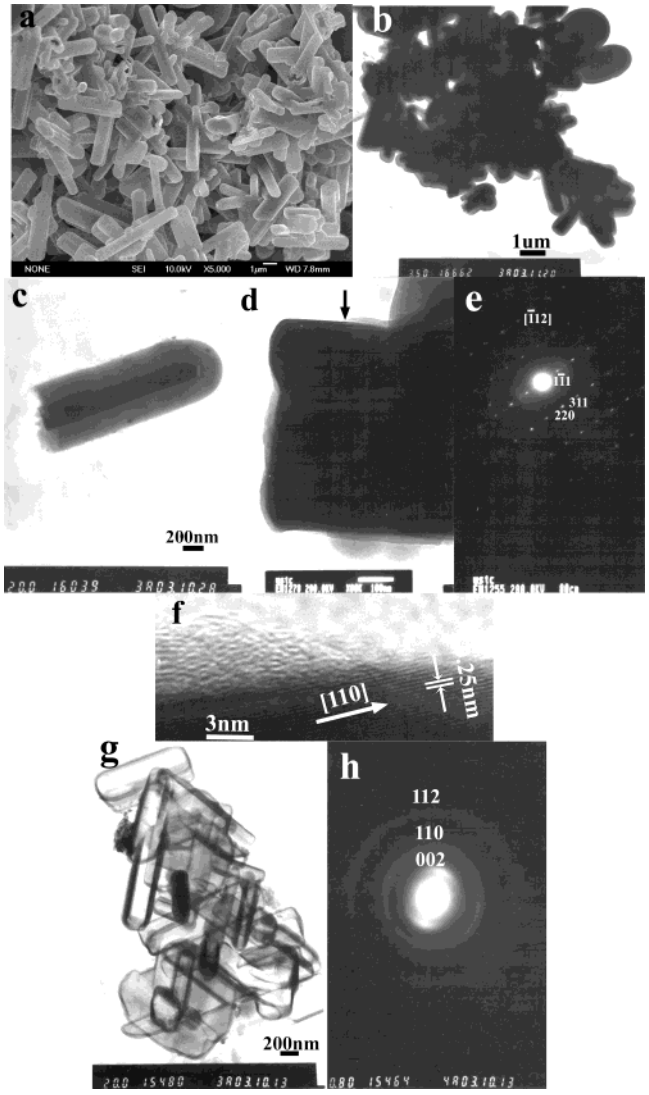

Figure 3. Typical FSEM, TEM, HRTEM images of the as-prepared CIOs and CMTs. (a) FSEM image. (b) TEM image. (C) A single CIO. (d) An end of an Fe_3O_4 nanowire partly coated by carbon (as arrowed) and over coated by carbon at the bottom (e) SAED pattern of the CIO shown in (d). (f) HRTEM image of the segment (as arrowed in (d), but the direction is left to right reversed). (g) TEM image of a single CIO coexisted with the CMTs. (h) A typical SAED pattern of a CMT.

for bulk Fe_3O_4 and Fe_3O_4 nanowires.[24,25] The broad lines of the magnetic sextets and the smooth inner slopes suggest the existence of a wide size distribution of the obtained IOs.

Field emission scanning electron microscopy (FSEM) and transmission electron microscopy (TEM) observations indicate that the products are composed of CIOs and solid spherical carbons, and the yield of the CIOs is about 65−70%. Figure 3a shows a typical FSEM image of the as-obtained CIOs. These CIOs are straight with a diameter range of 150−1500 nm and lengths up to 6 μm and with at least one closed end. The results of the FSEM-energy-dispersive X-ray analyses indicate that the average atomic ratio of elements C, Fe, O, and Cu is 26.82:3.00:3.97:0.28, and the atomic ratio of O/Fe (∼1.33) is consistent with that of the theoretical calculation result of Fe_3O_4, whereas the appearance of copper is due to the copper grid that supports the specimen. A typical TEM image of the products shown in Figure 3b indicates that the as-obtained CIOs were made of two parts, the outer part (carbon) coated on the interior IOs. Figure 3c shows a single Fe_3O_4 nanowire partly coated by carbon. An end of a single Fe_3O_4 nanowire partly

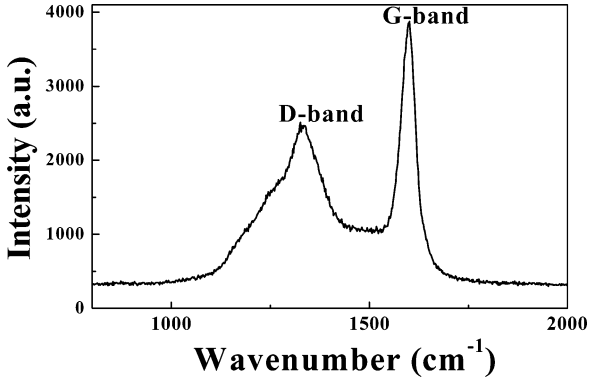

Figure 4. Typical Raman spectrum of the as-obtained CMTs.

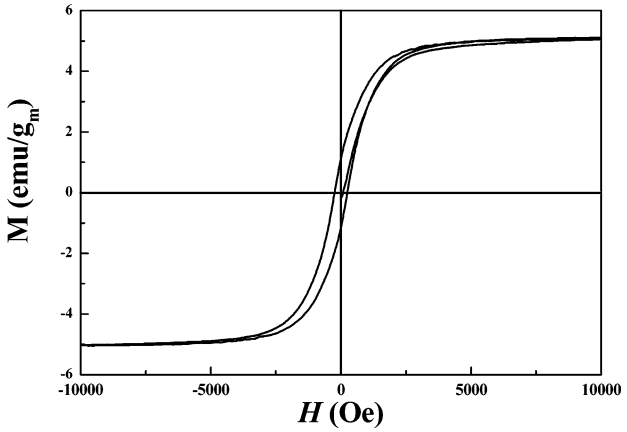

Figure 5. Magnetic hysteresis loop for the as-obtained CIOs at room temperature.

coated by carbon (as arrowed) and over coated by carbon at the bottom is shown in Figure 3d. Its selective area electron diffraction (SAED) pattern shown in Figure 3e can be indexed to be the [$\bar{1}$12] zone axis of the fcc Fe_3O_4. This pattern presents sharp diffraction spots, which can be indexed to (1$\bar{1}$1), (220), and (311) reflections from fcc Fe_3O_4. Besides these spots, we could only observe arcs from carbon 002 reflections. The SAED pattern of the Fe_3O_4 nanowire behaves as clear spots, not as rings, indicates that it has high crystallinity. The HRTEM image of a portion of a CIO composed of Fe_3O_4 and carbon (as arrowed in Figure 3d, but the direction is left to right reversed) is shown in Figure 3f. The interplanar spacing (0.25 nm) agrees very well with the lattice spacing between every {311} plane of fcc Fe_3O_4 crystal (0.253 nm). Combined with the SAED results, it is concluded that the growth direction [110] for the Fe_3O_4 nanowire is perpendicular to the (311) plane, which is consistent with the previous reports about IOs.[25] A great deal of HRTEM investigation on the Fe_3O_4 nanowires indicates that most of them prepared by this method are structurally uniform and perfect single crystallites, as evidenced by their regular set of lattice fringes and strong SAED patterns. However, the HRTEM image of the graphite layers on the surfaces of the Fe_3O_4 nanowire displays a disordered stacking feature, and the interior spacing of the adjacent graphite layers are usually different from each other, which indicated the low crystallinity of the carbon layers. Figure 3g shows a typical TEM image of the CMTs coexisted with only a single CIO obtained after HCl acid treatment. These straight CMTs with a diameter range of 200−400 nm and with one or two closed ends might be used as templates to prepare other materials encapsulated in CMTs. A typical SAED pattern of one CMT is shown in Figure 3h, its arcs and rings could be indexed as (002), (110), and (112) reflections for hexagonal carbon, which is also indicative of the low graphitic degree of the CMTs. The Raman spectrum of the as-obtained carbon microtubes is show in Figure 4, in which a broad peak at 1334 cm^{-1} as well as a sharp absorption peak at 1600 cm^{-1} can be clearly seen. The peak at 1334 cm^{-1} is usually associated with the vibrations of carbon atoms with dangling bonds for the in-plane terminations of disordered graphite and is labeled as the D-band, and the peak at 1600 cm^{-1} (G-band) (corresponding to the E_{2g} mode) is closely related to the vibration in all sp^2 bonded carbon atoms in a 2-dimensional hexagonal lattice, such as in a graphene layer.[26,27] The intensity ratio of the D to G band (I_D/I_G) is calculated to be 0.64, further reflecting the relative disorder and low graphitic crystallinity of the CMTs. This result coincides with that of XRD, SAED, and HRTEM analyses.

Figure 5 shows magnetic properties of the as-obtained products measured at room temperature. The hysteresis loop of the products shows a ferromagnetic behavior with saturation magnetization (M_s), remanent magnetization (M_r), and coercivity (H_c) values of ca. 5.11 emu/g, 1.14 emu/g, and 244.5 Oe, respectively, and the values of the M_s are much lower than those of the Fe_3O_4 nanowires.[25] Compared with the value ($H_c \approx 1$ Oe) of bulk iron, an enhancement of coercivity (244.5 Oe) for CIOs (Figure 3) was observed.

As it is known that ferrocene ($Fe-(Cp)_2$, Cp = C_5H_5) is a sandwich organometallic compound, the Fe−Cp bond is through the d-electrons of the metal and the π-electrons of the Cp groups, and this bond is generally less stable than the bonds in the Cp ring itself. With the increasing temperature, the Fe atoms decomposed from ferrocene will react with the O atoms decomposed from ethanol to form Fe_3O_4. At the end of this experiment, ferrocene and ethanol were converted into Fe_3O_4, C, H_2O, and residual gases. As no hollow carbon microtubes and Fe_3O_4 nanowires free of carbon were found before the HCl acid treatment process, and many of the as-obtained CIOs and CMTs have two closed ends, it is reasonable to speculate that Fe_3O_4 nanowires are formed at first in the whole formation process of CIOs and then carbons (decomposed from ethanol and/or from Cp rings) are coated on the surface of the Fe_3O_4 nanowires to diminish the surface energy produced by the IOs.[28,29] As the amount of carbons decomposed from both ferrocene and ethanol are in excess, they will continue to assemble on the surface of the IOs, and the original surface shell can continue to grow around the IOs. The velocities and densities of the carbons assembled on different surface areas of the IOs might be different, which ultimately results in the formation of partly or excessively carbon coated Fe_3O_4 nanowires. This process might be evidenced by the results of the TEM and HRTEM images (Figure 3); however, the exact formation mechanism of the as-obtained CIOs still needs further research.

Conclusions

In summary, a Co pyrolysis of an ethanol/ferrocene mixture in a stainless steel autoclave method was used to prepare straight Fe_3O_4 nanowires encapsulated in carbon microtubes. The encapsulated Fe_3O_4 nanowires are single crystalline with high crystallinity. Magnetic hysteresis loop measurements show that the CIOs display ferromagnetic properties at room temperature. Carbon microtubes were obtained after the interior Fe_3O_4 nanowires were dissolved by aqueous HCl acid solutions. This synthetic route for the encapsulation of Fe_3O_4 nanowire within a protective CMTs can perhaps be extended to produce many other desired materials inside CMTs.

Acknowledgment. Financial supports from the National Natural Science Found of China and the 973 Project of China are greatly appreciated. We thank Dr. Zhaoping Liu and Maosong Mo for informative discussions.

References and Notes

(1) Iijima, S. *Nature* **1991**, *354*, 56.
(2) Freemantle, M. *Chem. Eng. News* **1996**, *74*, 62.
(3) Sloan, J.; Cook, J.; Green, M. L. H.; Hutchison, J. L.; Tenne, R. *J. Mater. Chem.* **1997**, *7*, 1089.
(4) Saito, R.; Dresselhaus, M. S.; Dresselhaus, G. *Physical Properties of Carbon Nanotubes*; World Scientific Publishing: 1998.
(5) Harris, P. J. F. *Carbon Nanotubes and Related Structures-New Materials for the Twenty-First Century*; Cambridge University Press: 1999.
(6) Dresselhaus, M. S. In *Carbon Nanotubes*: *Synthesis, Structure, Properties and Applications*; Dresselhaus, G., Avouris, P., Eds.; Springer-Verlag: 2001.
(7) Ajayan, P. M.; Iijima, S. *Nature* **1993**, *361*, 333.
(8) Tsang, S. C.; Chen, Y. K.; Harris, P. J. F.; Green, M. L. H. *Nature* **1994**, *372*, 159.
(9) Terrones, M.; Hsu, W. K.; Schilder, A.; Terrones, H.; Grobert, N.; Hare, J. P.; Zhu, Y. Q.; Schwoerer, M.; Prassides, K.; Kroto, H. W.; Walton, D. R. M. *Appl. Phys. A: Mater. Sci. Process.* **1998**, *66*, 307.
(10) Bhabendra, K.; Pradhan, B. K.; Toba, T.; Kyotani, T.; Tomita, A. *Chem. Mater.* **1998**, *10*, 2510.
(11) Pradhan, B. K.; Kyotani, T.; Tomita, A. *Chem. Commun.* **1999**, *14*, 1317.
(12) Kyotani, T.; Tsai, L.-F.; Tomita, A. *Chem. Commun.* **1997**, *7*, 701.
(13) Hsu, W. K.; Hare, J. P.; Terrones, M.; Harris, P. J. F.; Kroto, H. W.; Walton, D. R. M.; Harris, P. J. F. *Nature* **1995**, *377*, 687.
(14) Schnitzler, M. C.; Oliveira, M. M.; Ugarte, D.; Zarbin, A. J. G. *Chem. Phys. Lett.* **2003**, *381*, 541.
(15) Kamalakaran, R.; Lupo, F.; Grobert, N.; Lozano-Castello, D. D.; Jin-Phillipp, N. Y.; Rühle, M. *Carbon* **2003**, *41*, 2737.
(16) Majetich, S. A.; Artman, J. O.; McHenry, M. E.; Nuhfer, N. T.; Staley, S. W. *Phys. Rev. B* **1993**, *48*, 16845.
(17) Jiang, L. Q.; Gao, L. *Chem. Mater.* **2003**, *15*, 2848.
(18) Crowley, T. A.; Ziegler, K. J.; Lyons, D. M.; Erts, D.; Olin, H.; Morris, M. A.; Holmes, J. D. *Chem. Mater.* **2003**, 15, 3518.
(19) Bao, J. C.; Tie, C. Y.; Xu, Z.; Suo, Z. Y.; Zhou, Q. F.; Hong, J. M. *Adv. Mater.* **2002**, *14*, 1483.
(20) Pham-Huu, C.; Keller, N.; Estournes, C.; Ehret, G.; Ledoux, M. J. *Chem. Commun.* **2002**, *17*, 1882.
(21) Rao, C. N. R.; Sen, R.; Satishkumar, B. C.; Govindaraj, A. *Chem. Commun.* **1998**, *15*, 1525.
(22) Satishkumar, B. C.; Govindaraj, A.; Vanitha, P. V.; Raychaudhuri, A. K.; Rao, C. N. R. *Chem. Phys. Lett.* **2002**, *362*, 301.
(23) Jang, J.; Yoon, H. *Adv. Mater.* **2004**, *15*, 2088.
(24) Evans, B. J.; Hafner, S. S. *J. Appl. Phys.* **1969**, *40*, 1411.
(25) Wang, J.; Chen, Q. W.; Zeng, C.; Hou, B. Y. *Adv. Mater.* **2004**, *16*, 137.
(26) Hu, G.; Cheng, M. J.; Ma, D.; Bao, X. H. *Chem. Mater.* **2003**, *15*, 1470.
(27) Dresselhaus, M. S.; Dresselhaus, G.; Pimenta, M. A.; Eklund, P. C. In *Analytical Applications of Raman Spectroscopy*; Pelletier, M. J., Ed.; Oxford: Blackwell Science; 1999; Chapter 9.
(28) Laurent, C.; Flahaut, E.; Peigney, A.; Rousset, A. *New. J. Chem.* **1998**, *11*, 1229.
(29) Dai, H.; Rinzler, A. G.; Nikolaev, P.; Thess, A.; Colbert, D. T.; Smalley, R. E. *Chem. Phys. Lett.* **1996**, *260*, 471.